Carcinogenesis vol.30 no.10 pp.1744–1753, 2009
doi:10.1093/carcin/bgp157
Advance Access publication June 23, 2009

Benzyl isothiocyanate-mediated generation of reactive oxygen species causes cell cycle arrest and induces apoptosis via activation of MAPK in human pancreatic cancer cells

Ravi P.Sahu, Ruifen Zhang, Sanjay Batra, Yan Shi and Sanjay K.Srivastava*

Department of Biomedical and Pharmaceutical Sciences and Cancer Biology Center, School of Pharmacy, Texas Tech University Health Sciences Center, Suite 1103, 1406 Coulter Drive, Amarillo, TX 79106, USA

*To whom correspondence should be addressed. Tel: +806 356 4750 ext. 224; Fax: +806 356 4770;
Email: sanjay.srivastava@ttuhsc.edu

In our previous studies, we have shown that benzyl isothiocyanate (BITC) inhibits the growth of human pancreatic cancer cells by inducing apoptosis. In the present study, we demonstrate the activation of all the three (MAPK) family members [extracellular signal-regulated protein kinase (ERK), c-jun N-terminal kinase (JNK) and P38] in response to BITC treatment. Exposure of Capan-2 cells with varying concentrations of BITC for 24 h resulted in the phosphorylation (activation) of ERK at Thr202/Tyr204, JNK at Thr183/Tyr185 and P38 at Thr180/Tyr182, leading to the induction of apoptosis. Similar MAPK activation was also observed in MiaPaCa-2 cells in response to BITC treatment. However, normal human pancreatic ductal epithelial cells did not show the activation of MAPK's and remained unaffected by BITC treatment. To confirm the role of ERK, JNK and P38 in BITC-induced G_2/M arrest and apoptosis, Capan-2 cells were pre-treated with MAPK-specific inhibitors or MAPK8-short hairpin RNA (shRNA) prior to BITC treatment. Significant protection from BITC-induced G_2/M arrest was observed in the cells pre-treated with MAPK kinase (MEK-1) but not JNK or P38 inhibitors. On the other hand, BITC-induced apoptosis was almost completely abrogated in the cells pre-treated with MEK-1, JNK or P38 inhibitors. Similarly, MAPK8-shRNA also offered almost complete protection against BITC-induced G_2/M arrest and apoptosis. Furthermore, we observed that BITC treatment leads to the generation of reactive oxygen species (ROS) in Capan-2 and MiaPaCa-2 cells, which in part was orchestrated by depletion of reduced glutathione (GSH) level. Blocking ROS generation with *N*-acetyl-L-cysteine (NAC) significantly prevented GSH depletion and activation of ERK and JNK but not P38. Further, NAC or tiron prevented G_2/M arrest by blocking G_2/M regulatory proteins and completely protected the cells from BITC-induced apoptosis. Taken together, our results suggest that BITC-mediated G_2/M arrest is mediated through ERK activation, whereas apoptosis is via ERK, JNK and P38.

Introduction

Pancreatic cancer is one of the most common human malignancies in both the gender and is the fourth leading cause of cancer-related deaths in the United States (1). It is estimated that ~38 000 people will be detected with pancreatic cancer per year and ~90% of them will die. The current treatment modalities used to treat pancreatic cancer patients are chemo and radiotherapies. The disease outcome from these treatments is not satisfactory as patients show a poor response to the therapy (2,3). Effective chemopreventive treatment would be a potential impact on pancreatic cancer morbidity and mortality. Currently, the emphasis on the use of dietary bioactive compounds is becoming an alternative, safe and striking approach to control and treat cancer. Recent findings from epidemiological, pharmacological and case control studies have indicated that isothiocyanates present in cruciferous vegetable have potential chemopreventive activity against several human malignancies including pancreatic cancer (4–7). Accumulating evidences from recent studies have shown the involvement of multiple signaling pathways in inducing cell death by isothiocyanates in different *in vitro* and *in vivo* experimental models (8–12). Benzyl isothiocyanate (BITC), a bioactive compound present in cruciferous vegetables such as garden cress, broccoli, etc. and widely consumed as part of our routine diet, has been reported to inhibit chemically induced human cancers in experimental animals (13–15). Previously, we have shown that BITC suppresses the growth of human pancreatic cancer cells by causing DNA damage, G_2/M cell cycle arrest and apoptosis (16) and in part this effect is mediated by the inhibition of nuclear factor kappa B activation (12); however, the exact mechanism underlying the role of BITC-mediated apoptosis in human pancreatic cancer has not been fully elucidated.

The present study thus aimed to investigate the mechanism by which BITC inhibits the growth of Capan-2 and MiaPaCa-2 pancreatic cancer cells. Our results indicate that activation of extracellular signal-regulated protein kinase (ERK) by BITC treatment results in cell cycle arrest and apoptosis, whereas activation of c-jun N-terminal kinase (JNK) and P38 were involved in apoptosis only. Further, we found that reactive oxygen species (ROS) are generated by BITC treatment leading to activation of ERK and JNK but not P38 and that ROS are generated due to depletion of glutathione (GSH) level. Pharmacologically or genetically inhibiting ERK, JNK or P38 activation or blocking ROS generation by antioxidant *N*-acetyl-L-cysteine (NAC) completely blocks BITC-mediated G_2/M cell cycle arrest and apoptosis. Interestingly, none of the above-mentioned effects were observed in the normal pancreatic epithelial cells in response to BITC treatment.

Abbreviations: APF, aminophenyl fluorescein; BITC, benzyl isothiocyanate; Cdc25C, cell division cycle 25C; Cdk1, cyclin-dependent kinase-1; DMSO, dimethyl sulfoxide; ELISA, enzyme-linked immunosorbent assay; ERK, extracellular signal-regulated protein kinase; FBS, fetal bovine serum; GSH, glutathione; GSSG, oxidized GSH; HPDE-6, human pancreatic ductal epithelial cells; hROS, highly reactive oxygen species; JNK, c-jun N-terminal kinase; MAPK, mitogen-activated protein kinase; MEK-1, MAPK kinase; NAC, *N*-acetyl-L-cysteine; PARP, poly (ADP-ribose) polymerase; PSN, penicillin-streptomycin-neomycin; ROS, reactive oxygen species; shRNA, short hairpin RNA; SOD, superoxide dismutase.

Materials and methods

Chemicals

BITC, RNAase I, sulforhodamine B, superoxide dismutase (SOD), catalase, tiron and antibodies against β-actin were purchased from Sigma-Aldrich, St Louis, MO. Keratinocyte-serum free medium and chemicals for cell culture such as epidermal growth factor, bovine pituitary extract, trypsin inhibitor, penicillin-streptomycin-neomycin (PSN) antibiotic mixture (PSN), sodium pyruvate and 4-(2-hydroxyethyl)-1-piperazineethanesulfonic acid buffer were purchased from Gibco BRL, Carlsbad, CA. mitogen-activated protein kinase (MAPK) kinase (MEK-1) (PD98059), JNK (SP600125) and P38 (SB202190) inhibitors were from Calbiochem, EMD Biosciences, Darmstadt, Germany, and GSH Kit from Cayman Chemical Company, Ann Arbor, MI. Fluoro H_2O_2 and highly reactive oxygen species (hROS) detection kit was from Cell Technology, Mountain View, CA. MAPK8-short harpin RNA (shRNA) was purchased from SuperArray, Frederick, MD. Heat-inactivated fetal bovine serum (FBS), horse serum and McCoy's 5A medium were purchased from Mediatech Cell Grow, Lawrence, KA. Cell Death Detection Apoptosis enzyme-linked immunosorbent assay (ELISA) kit was purchased from Roche Applied Science, Mannheim, Germany. Electrophoresis reagents were from Amresco, Solon, OH. Western blotting enhanced chemiluminescence reagent was purchased from Perkin Elmer, Waltham, MA. GSH was measured by using GSH Assay Kit from Cayman Chemical. Antibodies against cyclin B1, Cdc-2, phospho-Cdc-2 (Tyr-15), cell division cycle 25C (Cdc25C), phospho-Cdc25C (Ser-216), phospho-H2A.X (Ser139), phospho-ERK (Thr202/Thy204), ERK, phospho-JNK (Thr183/Tyr185), JNK, phospho-P38, P38, cleaved fragments of caspase-3 and poly (ADP-ribose) polymerase (PARP) were from Cell Signaling Technology, Danvers, MA.

Cell culture and proliferation assays

Capan-2 and MiaPaCa-2 cells were obtained from American type cell culture. Monolayer culture of Capan-2 cells were maintained in McCoy's medium supplemented with 10% FBS and 1% (v/v) antibiotics (PSN) in a humidified incubator with 5% CO_2 and 95% air. MiaPaCa-2 cells were maintained in Dulbecco's modified Eagle's medium supplemented with 4 mM L-glutamine and adjusted to contain 4.5 g/l glucose, 1.5 g/l sodium bicarbonate, 10% FBS, 2.5% horse serum (Mediatech) and 1% (v/v) antibiotics (PSN). Normal human pancreatic duct epithelial cells (HPDE-6) were a generous gift from Dr Ming-Sound Tsao, University of Toronto, Toronto, Canada (17). HPDE-6 cells were cultured in keratinocyte-serum free medium supplemented with 4 mM L-glutamine and adjusted to contain 0.2 ng/ml epidermal growth factor, 30 μg/ml bovine pituitary extract and 1% (v/v) PSN as described previously (17). Stock solution of BITC was prepared in 100% dimethyl sulfoxide (DMSO) and subsequently diluted in medium so that the final concentration of DMSO was 0.1% in the medium. The cells were treated with varying concentrations of BITC (0, 2.5, 5, 10 and 20 μM) for 24 h. In a time-dependent experiment, Capan-2 cells were treated with 10 μM BITC for 1, 3, 6, 12 and 24 h.

Cell cycle analysis

The effect of BITC on cell cycle distribution was assessed by flow cytometry after staining the cells with propidium iodide. Briefly, 0.3×10^6 cells were plated in T-25 flask in 3 ml medium and allowed to attach overnight. The medium was replaced with fresh medium and then the cells were pre-treated with (i) 50 μM MEK-1 (PD98059), 30 μM JNK (SP600125) or 20 μM P38 (SB202190) inhibitors for 1 h, (ii) 5 mM NAC for 1 h and (iii) 5 mM GSH, 5000 U/ml catalase, 5000 U/ml SOD or 10 mM tiron for 1 h followed by treatment with or without 10 μM BITC for 24 h. Control cells were treated with 0.1% DMSO only. After incubation of cells at 37°C for specified time, floating and adherent cells were collected by using 0.05% trypsin, washed twice with cold phosphate-buffered saline and fixed with ice-cold 70% ethanol overnight at 4°C. The cells were then treated with 80 mg/ml RNase A and 50 mg/ml propidium iodide for 30 min. The stained cells were analyzed using a Coulter Epics XL Flow Cytometer. Approximately 20 000 cells were evaluated for each experiment. In all determinations, cell debris and clumps were excluded from the analysis. The cell cycle data were reanalyzed using MODFIT software.

MAPK8-shRNA transfection

The effect of BITC-induced apoptosis mediated by the activation of MAPK was confirmed by transfecting Capan-2 cells with MAPK8-shRNA (SuperArray). MAPK8-shRNA causes the silencing of all the three members of MAPK family (ERK, JNK and P38). Briefly, 3×10^5 Capan-2 cells in 10 ml McCoy's medium were plated in 100 mm culture dish followed by transfection with 2 μg of MAPK-shRNA plasmid diluted in Opti-minimum essential medium serum-free medium to which lipofectamine reagent was added before the mixture was added to cells. Subsequently, cells were incubated with plasmid–lipofectamine mixture for 5 h and replenished with normal growth medium for 48 h. After transfection, cells were treated either with 0.1% DMSO or with 10 μM BITC for 24 h and were processed for cell cycle analysis or western blotting. Cell lysates were prepared and 20 μg of protein was analyzed by western blotting. The same blots were stripped and reprobed with anti-actin antibody for equal loading. Each immunoreactive bands were quantitated and corrected with actin and the ratios of phopho-ERK, phospho-JNK and phopho-P38 with their respective total ERK, JNK and P38 protein levels were presented as bar diagram.

Western blot analysis

About 1×10^6 Capan-2, MiaPaCa-2 and HPDE-6 cells in 10 ml medium were plated in 100 mm culture dish and treated with varying concentrations of BITC (0, 2.5, 5, 10 and 20 μM) for 24 h. In a separate experiment, Capan-2 cells were pre-treated (i) with 50 μM MEK-1 (PD98059), 30 μM JNK (SP600125) or 20 μM P38 (SB202190) inhibitors and (ii) with 5 mM NAC for 1 h followed by treatment with 10 μM BITC for 24 h. Whole-cell extracts were prepared as described by us previously (16,18). Lysates containing 20–40 μg of proteins were subjected to Sodium dodecyl sulfate–polyacrylamide gel electrophoresis and proteins were transferred onto polyvinylidene difluoride membrane. After blocking with 5% non-fat dry milk, the membrane was incubated overnight with the desired primary antibody (1:1000 dilution). Subsequently, the membrane was incubated with appropriate secondary antibody and the immunoreactive bands were visualized using enhanced chemiluminescence kit according to the manufacturer's instructions. The same membrane was reprobed with the antibody against actin (1:50 000 dilution) as an internal control for equal protein loading.

Generation of ROS

The generation of ROS was evaluated by measuring the levels of hydrogen peroxide produced in the cells using Fluorescent Hydrogen Peroxide/Peroxidase Detection Kit (Cell Technology) according to user's manual with slight modification. The fluoro H_2O_2 detection kit utilizes a non-fluorescent detection reagent to detect H_2O_2. H_2O_2 oxidizes the detection reagent in a 1:1 stoichiometry to produce a fluorescent product resorufin which is catalyzed by peroxidase in a homogeneous no-wash assay system. Briefly, 40 000 Capan-2, MiaPaCa-2 or HPDE-6 cells were plated in 96 well plates in 100 μl medium and allowed to attach overnight. To evaluate the generation of ROS in a time-dependent manner, cells were treated with 10 μM BITC for 0.5, 1, 2, 4 and 6 h. In a separate experiment, cells were treated with 0, 2.5, 5, 10 and 20 μM BITC for 2 h. After the completion of BITC treatment for indicated time points, cells were washed twice with their respective plain mediums (without 10% FBS) followed by incubation with 100 μl reaction cocktail (10 mM detection reagent, 10 U/ml horseradish peroxidase in plain medium) for 10 min at room temperature in dark. After incubation, the fluorescence was measured at excitation 540 nm and emission 595 nm in a fluorescent plate reader. ROS generation was also evaluated by measuring the levels of hydrogen peroxide produced in the cells by flow cytometry. Levels of hydrogen peroxide in control and BITC-treated Capan-2 cells were determined by staining the cells with 6-carboxy-2′,7′-dichlorodihydrofluoroscein diacetate as described by us previously (19,20). 6-Carboxy-2′,7′-dichlorodihydrofluoroscein diacetate is a cell permeable probe and is cleaved by non-specific esterases and oxidized by peroxides produced in the cells to form fluorescent 2′,7′-dichlorofluoroscein. The intensity of 2′,7′-dichlorofluoroscein fluorescence is proportional to the amount of peroxide produced in the cells. Briefly, 0.5×10^6 cells were plated in 25 cm^2 flasks and allowed to attach overnight. After treatment with BITC, cells were further incubated with 5 μM 6-carboxy-2′,7′-dichlorodihydrofluoroscein diacetate at 37°C for 15 min. Subsequently, cells were washed and re-suspended in phosphate-buffered saline and analyzed for 2′,7′-dichlorofluoroscein fluorescence by using Coulter XL flow cytometer. Approximately 20 000 cells were evaluated for each experiment. In all determinations, cell debris and clumps were excluded from the analysis.

Generation of hROS

The generation of other ROS by BITC treatment was measured using hROS detection kit (Cell Technology) according to user's manual with slight modification. This kit detects hROS [hydroxyl radical (·OH)], peroxynitrite ($ONOO^-$) and hypochlorite (^-OCl) production in the cells using a novel probe, aminophenyl fluorescein (APF). APF is a cell permeable non-fluorescent probe that oxidizes by hROS into strongly fluorescent APF. This probe has little reactivity toward other ROS such as singlet oxygen (O_2^1), superoxide ($O_2^{-}\cdot$), H_2O_2, nitric oxide (NO·) and alkyl peroxide ($RO_2\cdot$). Briefly, 40 000 Capan-2, MiaPaCa-2 or HPDE-6 cells were plated in 96 well plates in 100 μl medium and allowed to attach overnight. After that cells were rinsed with modified Hanks balanced salt solutions buffer supplemented with 10 mM 4-(2-hydroxyethyl)-1-piperazineethanesulfonic acid, 1 mM $MgCl_2$, 2 mM $CaCl_2$ and 2.7 mM glucose followed by incubation with 10 μM APF (diluted in modified Hanks balanced salt solutions buffer in 1:10 ratio) for 60 min at 37°C. After incubation with APF, to evaluate the generation of ROS in a time-dependent manner, cells were treated with 10 μM BITC for 0.5, 1, 2, 4 and 6 h. In a separate experiment, cells were treated with 0, 2.5, 5, 10 and 20 μM BITC for 2 h followed by measurement of fluorescence at excitation 488 nm and emission 515 nm in a fluorescent plate reader.

Apoptosis determination

Apoptotic cell death was measured by analysis of caspase-3 and PARP cleavage and by Cell Death Detection Apoptosis ELISA method as described by us previously (18). This assay is based on a quantitative sandwich-enzyme-immunoassay principle using monoclonal antibodies directed against DNA and histones. Briefly, Capan-2 and HPDE-6 cells were seeded in 96 well plate in 100 μl of their respective medium and treated with 0, 2.5, 5, 10 and 20 μM BITC for 24 h, whereas control cells received DMSO only. Cell lysates were added to the plate coated with streptavidin and then mixed with biotinylated anti-histone antibodies and peroxide-conjugated anti-DNA antibodies and the plates were read at 405 and at 490 nm for blank on EL800 ELISA plate reader, Bio-Tek Instruments, Winooski, VA. Each sample was analyzed in triplicate and the average values were subtracted from the background values.

Determination GSH and oxidized GSH levels

The effect of BITC treatment on GSH level was evaluated using a commercial kit (Cayman Chemical Co.). Briefly, 1×10^4 Capan-2 or HPDE-6 cells in 0.1 ml medium were plated in 96 well plate and treated with DMSO or 10 μM BITC for 1, 2 or 3 h. In a separate experiment, cells were pre-treated with 5 mM NAC for 1 h prior to treatment with BITC for 2 h. Cells were lysed with 1× Hanks balanced salt solutions and sonicated by eight pulses and centrifuged at 10 000*g* for 10 min. Protein in control and treated samples was equalized and then deproteinated with equal volume of 10% metaphosphoric acid. Samples were collected and the supernatant was used for GSH and oxidized GSH (GSSG) measurements using GSH Assay Kit (Cayman Chemical) following the manufacturer's protocol. This assay kit used an optimized enzymatic

recycling method using GSH reductase for the quantification of cellular GSH content. In another experiment, GSH was masked by 2-vinylpyridine for 1 h before the assay to determine the GSSG levels in the samples. The samples were read at 405 nm at 5 min intervals for 30 min. The GSH and GSSG were determined by comparison with standards and normalized to protein content.

Densitometric scanning and statistical analysis

The intensity of immunoreactive bands was determined using a densitometer (Molecular Dynamics, Sunnyvale, CA) equipped with Image QuaNTsoftware. Results are expressed as mean ± standard error of the mean of two to three independent experiments, each conducted in triplicate. Data were analyzed by one-way analysis of variance followed by Bonferroni's post hoc analysis for multiple comparisons. All statistical calculations were performed using InStat software and GraphPad Prism 4.0. Differences were considered statistically significant at $^{*}P < 0.05$, $^{**}P < 0.01$ and $^{***}P < 0.001$ when compared with control and $\#P < 0.05$, $\#\#P < 0.01$ and $\#\#\#P < 0.001$ when compared with BITC treatment.

Results

BITC treatment causes activation of MAPK pathway

In our previous studies, we have shown that BITC induces cell cycle arrest and apoptosis by causing DNA damage (16). In the present study, we investigated the molecular mechanism responsible for BITC-induced G_2/M cell cycle arrest and apoptosis. Previous studies have indicated the involvement of MAPK in initiating G_2/M cell cycle arrest in prostate cancer cells (21,22), instigating us to see if cell cycle arrest in our model was due to MAPK activation. We observed that BITC treatment in Capan-2 cells resulted in the substantial activation of ERK at Thr202/Thy204, JNK at Thr183/Tyr185 and P38 at Thr180/Tyr182 by activating phosphorylation in a concentration-dependent manner (Figure 1A). The activation of ERK and JNK was as early as 1 h after BITC treatment and was sustained throughout the duration of the experiment (Figure 1B). On the other hand, activation of P38 was observed around 24 h of BITC treatment (Figure 1B). In addition, we observed activation of Bax and cleavage of caspase-3 and PARP in response to BITC treatment (Figure 1A). The activation of Bax and cleavage of caspase-3 and PARP was pronounced at 12 and 24 h of BITC treatment in Capan-2 cells (Figure 1B).

Role of MAPK activation in BITC-mediated cell cycle arrest and apoptosis

To confirm the involvement of ERK, JNK and P38 in BITC-induced G_2/M cell cycle arrest and apoptosis, Capan-2 cells were pre-treated with MEK-1 inhibitor (PD98059), JNK inhibitor (SP600125), P38 inhibitor (SB202190) or MAPK8-shRNA followed by treatment with BITC. Our results demonstrate that pre-treatment of Capan-2 cells with MEK-1 inhibitor PD98059 significantly abrogated BITC-induced G_2/M cell cycle arrest (Figure 2A) and apoptosis (Figure 2B) in a concentration-dependent study. Although, BITC-mediated activation of JNK and P38 was almost completely blocked in the cells pre-treated with JNK or P38 inhibitors as evaluated by western blotting (Figure 2C and D), both JNK (SP600125) and P38 (SB202190) inhibitors failed to protect the cells from BITC-mediated G_2/M cell cycle arrest (data not shown). Further, MEK-1 inhibitor blocked BITC-mediated activation of ERK as well as down-regulation of G_2/M regulatory proteins such as cyclin-dependent kinase-1 (Cdk1), cyclin B1, Cdc25C and cleavage of caspase-3 and PARP (Figure 2E), suggesting the involvement of ERK in BITC-induced G_2/M cell cycle arrest and apoptosis. BITC-mediated apoptosis was almost completely abrogated in the cells pre-treated with ERK, JNK or P38 inhibitors as evaluated by cell death apoptosis ELISA assay (Figure 2F).

In order to further confirm the role of MAPK in mediating cell cycle arrest and apoptosis by BITC treatment, we used MAPK8-shRNA to silence the activation of MAPK. Transfection of Capan-2 cells with MAPK8-shRNA prior to BITC treatment resulted in the significant silencing of the activation of ERK, JNK and p38 (Figure 3A). Intriguingly, ERK and JNK levels were higher in cells transfected with MAPK8-shRNA alone compared with control cells. It is possible that cells undergo stress during transfection leading to the activation of ERK and JNK, which are known to be responsive to stress. However, activation of ERK or JNK by BITC treatment was of much higher magnitude and was attenuated by MAPK8-shRNA to the level of MAPK8-shRNA transfection alone (Figure 3A). Further, MAPK8-shRNA completely protected Capan-2 cells from BITC-induced G_2/M

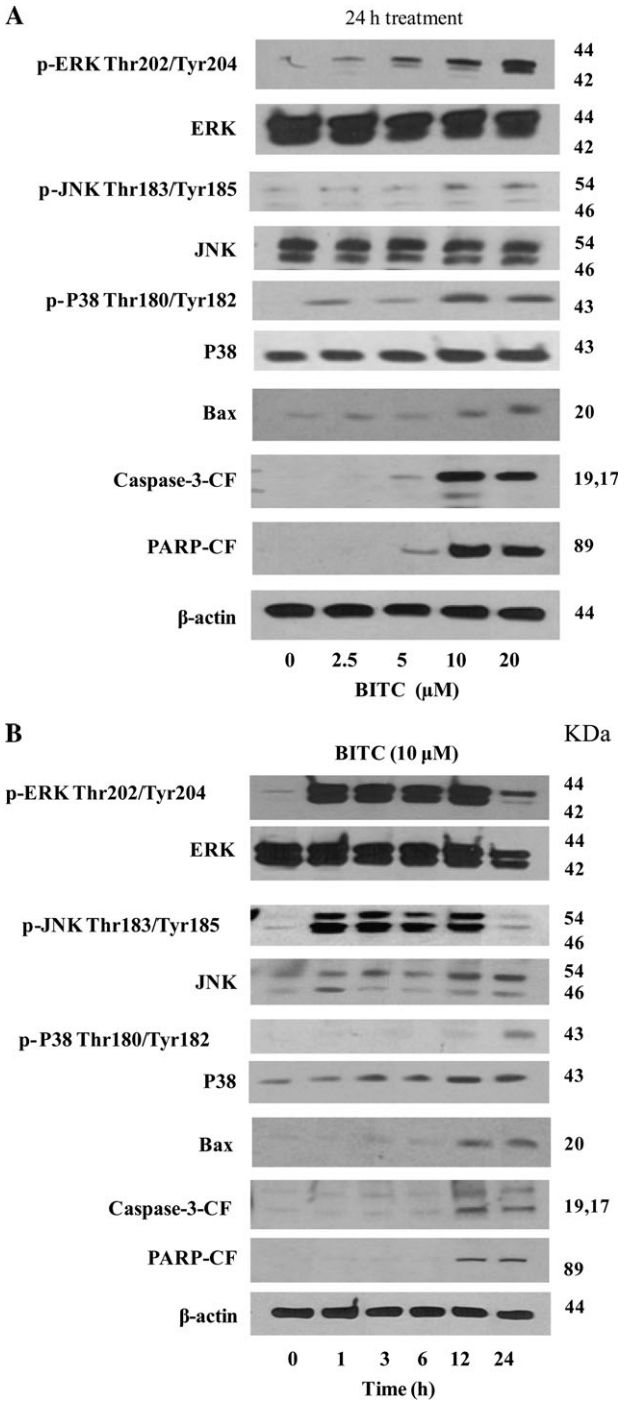

Fig. 1. BITC treatment causes activation of MAPK. (**A**) Capan-2 cells were treated with different concentrations of BITC for 24 h or (**B**) for different time intervals with 10 μM BITC. Cells were lysed and total lysate was prepared as described in Materials and Methods. Representative immunoblots show the effect of BITC treatment on the phosphorylation of ERK (Thr202/Tyr204), JNK (Thr183/Thr185) and P38 (Thr180/Tyr182) as well as protein levels of ERK, JNK, P38 and Bax and cleavage of caspase-3 and PARP. Each blot was stripped and reprobed with anti-β-actin antibody to ensure equal protein loading.

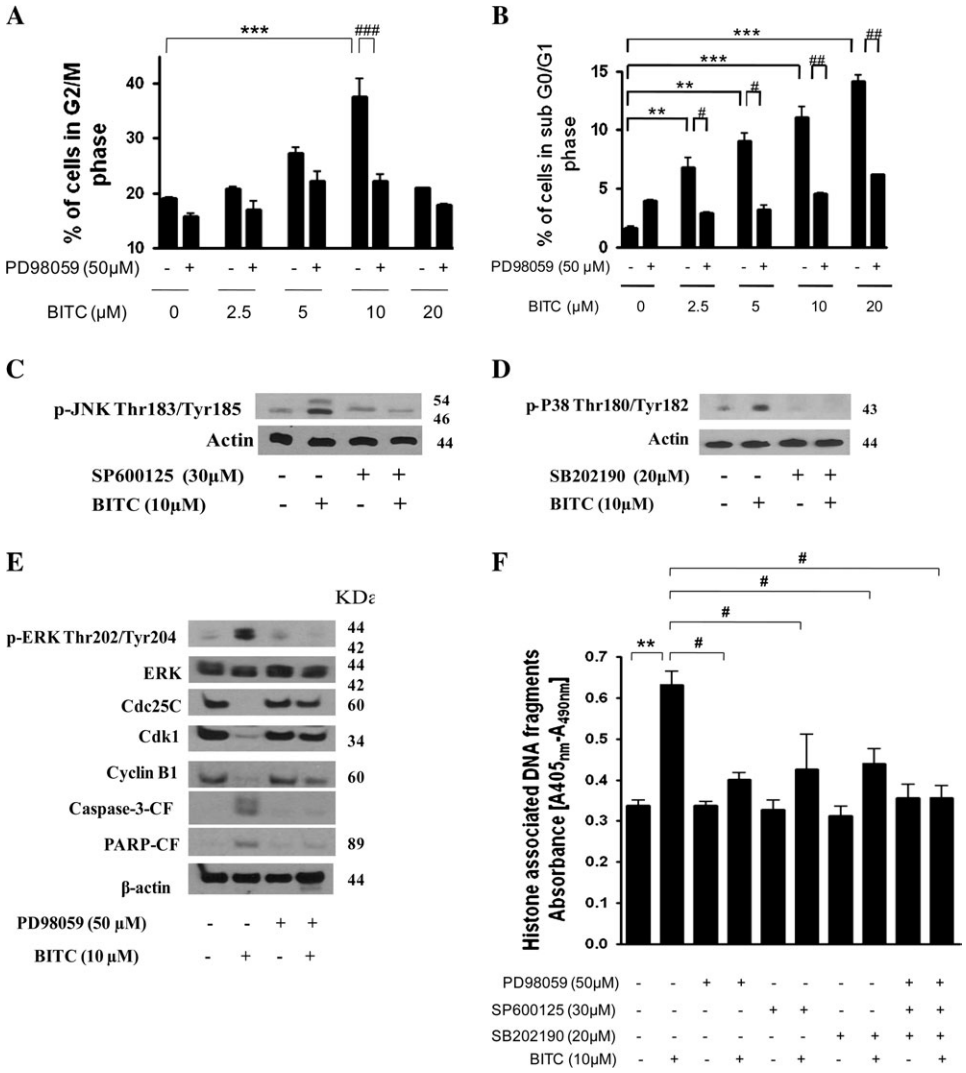

Fig. 2. Pharmacologically inhibiting MAPK blocks BITC-mediated G_2/M cell cycle arrest and apoptosis. (**A**) Capan-2 cells were pre-treated with 50 μM MEK-1 inhibitor PD98059 for 1 h followed by treatment with or without 2.5–10 μM BITC for 24 h and its effect on the cell cycle distribution and (**B**) apoptosis was evaluated by flow cytometry as described in Materials and Methods. Capan-2 cells were pre-treated with (**C**) 30 μM JNK inhibitor (SP600125) or (**D**) 20 μM p38 inhibitor (SB202190) and then treated with 10 μM BITC for 24 h. The phosphorylation of JNK and p38 was evaluated by western blotting. (**E**) Immunoblotting against p-ERK (Thr202/Tyr204), ERK, Cdc25C, Cdk1, cyclin B1 and the cleaved caspase-3 and PARP. Each blot was stripped and reprobed with anti-β-actin antibody to ensure equal protein loading. (**F**) The effects of MEK-1 (PD98059; 50 μM), JNK (SP600125; 30 μM) and P38 (SB202190; 20 μM) inhibitors on apoptosis were also evaluated by Cell Death Detection Apoptosis ELISA assay as described in Materials and Methods. Values are means ± standard errors of the mean of three independent experiments (each conducted in triplicate). Data were analyzed by non-parametric one-way analysis of variance followed by Bonferroni's post hoc multiple comparison test. Differences were considered statistically significant at $^{*}P < 0.05$, $^{**}P < 0.01$ and $^{***}P < 0.001$ when compared with control and $\#P < 0.05$, $\#\#P < 0.01$ and $\#\#\#P < 0.001$ when compared with BITC treatment.

arrest (Figure 3B) and apoptosis (Figure 3C). MAPK8-shRNA also blocked the down-regulation of Cdk1, cyclin B1 and Cdc25C, activation of Bax and cleavage of caspase-3 and PARP mediated by BITC treatment (Figure 3D). Blocking BITC-mediated Bax expression by MAPK8-shRNA also indicates that Bax is regulated by MAPK and may be acting as an intermediate molecule in inducing apoptosis in Capan-2 cells; however, further studies are needed to substantiate this assumption. Taken together, these results suggest the involvement of ERK in BITC-mediated cell cycle arrest and apoptosis, whereas JNK and P38 in BITC-induced apoptosis.

BITC treatment causes ROS generation

Next, we wanted to investigate the mechanism of MAPK activation by BITC treatment. Previous studies including those from our laboratory have indicated the involvement of ROS in inducing apoptosis by different mechanisms including the activation of ERK (19,20,23–26). We therefore sought to determine whether BITC treatment causes generation of ROS in our model. Our results show that BITC causes significant generation of ROS in Capan-2 cells as quantitated by using a commercially available kit that specifically measures hydrogen peroxide (Figure 4A). The generation of ROS was as early as 0.5 h after BITC treatment (Figure 4B). To see if BITC causes the generation of highly ROS other than hydrogen peroxide, we used a kit which measures the generation of singlet oxygen (O_2^1), superoxide ($O_2^{-}\cdot$), nitric oxide (NO·), hydroxyl (·OH) and alkyl peroxide ($RO_2\cdot$) radicals collectively called hROS. We observed a modest increase in the generation of hROS in response to BITC treatment (Supplementary Figure 1 is available at *carcinogenesis* online). To establish the association of ROS with the activation of ERK/JNK/P38 and apoptosis by BITC, cells were pre-treated with antioxidant NAC prior to BITC treatment. We observed that BITC-induced ROS generation was completely

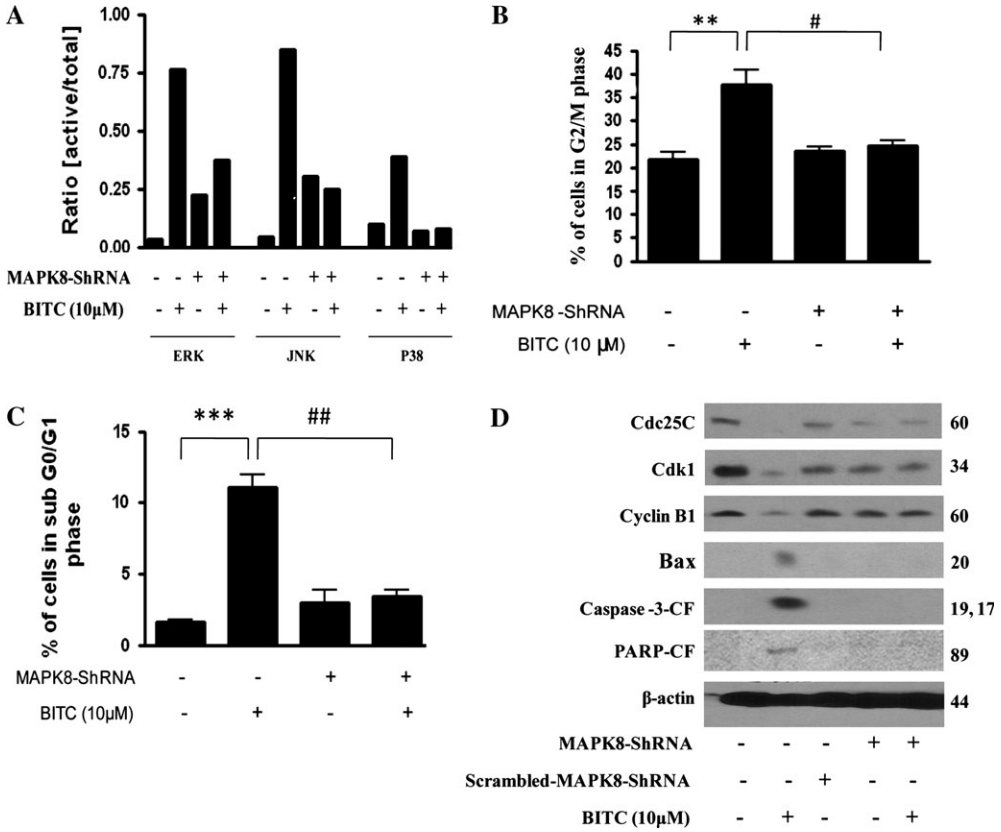

Fig. 3. Silencing MAPK by MAPK8-shRNA abrogates BITC-induced G_2/M arrest and apoptosis. The effect of BITC was evaluated after silencing the activation of ERK, JNK and p38 using a general MAPK8-shRNA. Capan-2 cells were transfected with MAPK8-shRNA for 48 h and treated with 10 μM BITC for 24 h and analyzed by western blotting or cell cycle analysis by flow cytometry. (**A**) The blots were probed with p-ERK, ERK, p-JNK, JNK, p-p38, p38 and actin. Each immunoreactive bands were quantitated and corrected for equal protein loading and the ratio of p-ERK/ERK, p-JNK/JNK and p-p38/p38 was determined. Transfected and BITC-treated cells were further analyzed by flow cytometry for (**B**) cell cycle analysis, (**C**) apoptosis or (**D**) expression of G_2/M regulatory proteins Cdc25C, Cdk1, cyclin B1, Bax, caspase-3 and PARP by western blotting. Each blot was stripped and reprobed with anti-β-actin antibody to ensure equal protein loading. Values are means ± standard errors of the mean of three independent experiments (each conducted in triplicate). Data were analyzed by non-parametric one-way analysis of variance followed by Bonferroni's post hoc multiple comparison test. Differences were considered statistically significant at $^{*}P < 0.05$, $^{**}P < 0.01$ and $^{***}P < 0.001$ when compared with control and $\#P < 0.05$ and $\#\#P < 0.01$ when compared with BITC treatment.

blocked by NAC treatment (Figure 4C). Further, BITC-mediated G_2/M arrest was significantly prevented in the cells pre-treated with NAC (Figure 4D). Moreover, activation of ERK at Thr202/Tyr204 and JNK at Thr183/Tyr185 was almost completely blocked when pre-treated with NAC (Figure 4E). However, NAC treatment failed to block the activation of P38 (data not shown). NAC pre-treatment also blocked the phosphorylation of H2A.X, induction of P21 and degradation of Cdc25C mediated by BITC (Figure 4E). BITC-mediated decrease in Cdk1 and cyclin B1 levels were also prevented by NAC pre-treatment (Figure 4E). In addition, NAC treatment completely protected Capan-2 cells from BITC-induced apoptosis (Figure 4E and F) by blocking the cleavage of caspase-3 and PARP (Figure 4E).

BITC causes depletion in GSH levels

Intracellular generation of ROS is generally due to increased oxidative stress caused by imbalance in cellular redox homeostasis (27). Reduced GSH is known to maintain redox balance (27). Thus, in order to delineate the mechanism of ROS generation by BITC in Capan-2 cells, we measured intracellular GSH levels. Our results demonstrate that 10 μM BITC treatment within 2 h significantly increased GSSG/GSH ratio and depleted total GSH levels (Figure 5A and C), which was completely prevented when pre-treated with NAC (Figure 5B and C). These results suggest that depletion of antioxidant GSH by BITC could be a possible reason for the perturbation in cellular redox homeostasis leading to increased levels of ROS. Further to establish that the depletion of GSH is the key factor in BITC-induced ROS generation-mediated G_2/M cell cycle arrest, cells were pre-treated with 5 mM GSH followed by the treatment with 10 μM BITC. Our results demonstrate that GSH pre-treatment completely protected the cells from BITC-mediated G_2/M cell cycle arrest (Figure 5D). Catalase, SOD and tiron have been shown to scavenge ROS (28,29). In order to determine whether ROS scavengers other than NAC can block BITC-mediated G_2/M cell cycle arrest, cells were pre-treated with catalase, SOD or tiron followed by treatment with 10 μM BITC for 24 h. As shown in Figure 5D, BITC-mediated G_2/M arrest was significantly abrogated in the cells pre-treated with catalase, SOD or tiron, confirming the role of ROS in BITC-induced G_2/M arrest (Figure 5D).

Effect of BITC on MiaPaCa-2 and normal pancreatic HPDE-6 cells

To rule out the possibility that the observed effects of BITC are not specific to Capan-2 cells, we also evaluated the effect of BITC on MiaPaCa-2 human pancreatic cancer cells. We have shown previously that BITC treatment suppresses the proliferation of MiaPaCa-2 cells (18). Similar to our observations made in Capan-2 cells, 10 μM BITC treatment caused early and significant ROS generation in MiaPaCa-2 cells in a time-dependent study (Figure 6A). BITC treatment caused significant G_2/M arrest (Figure 6B) and apoptosis (Figure 6C) in a concentration-dependent manner. In addition, we observed that BITC treatment resulted in the phosphorylation (activation) of ERK (Thr202/Tyr204), JNK (Thr183/Tyr185) and p38 (Thr180/Tyr182) as well as cleavage of caspase-3 and PARP (Figure 6D), suggesting the mechanism similar to what we observed in Capan-2 cells. We further

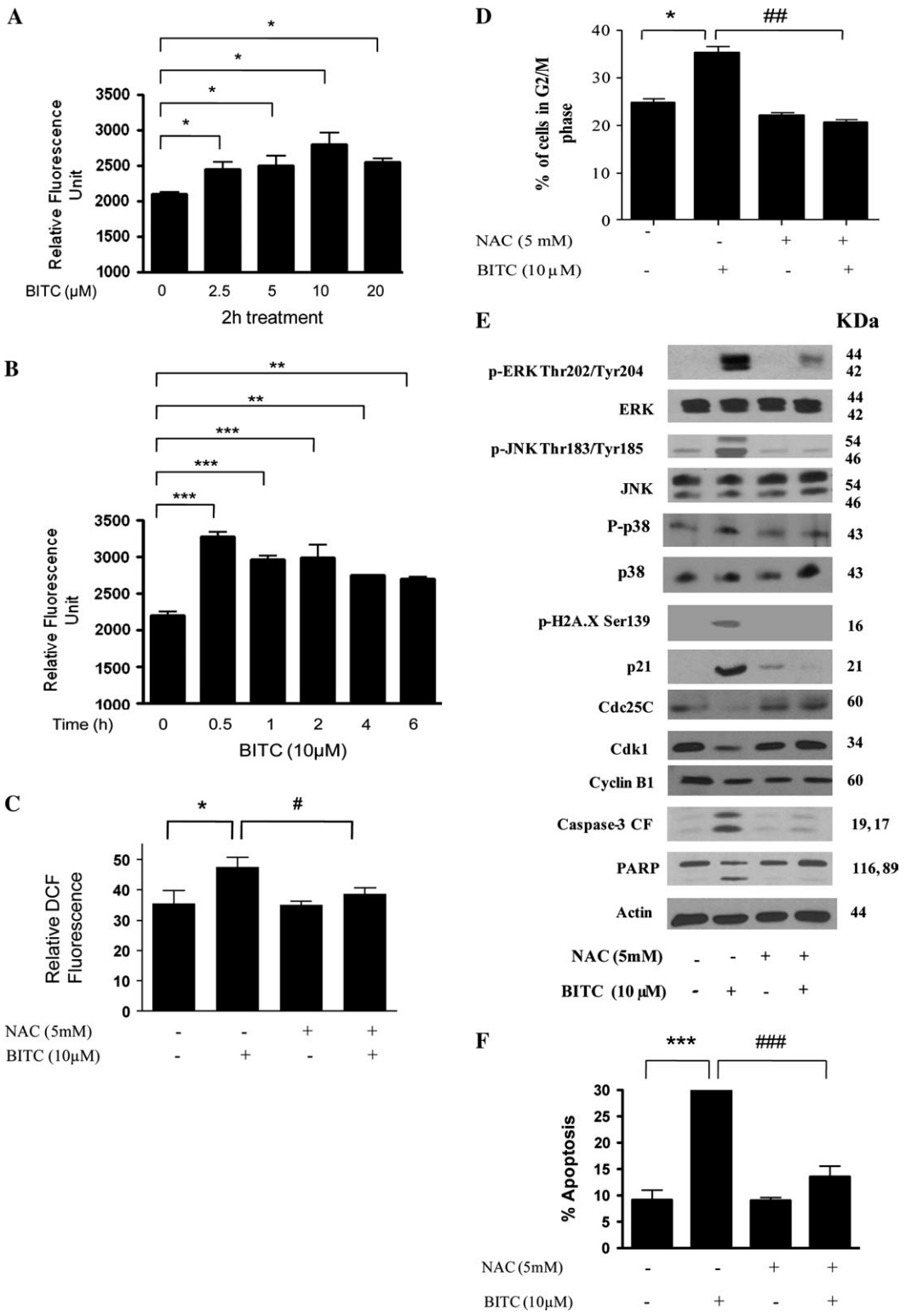

Fig. 4. Involvement of ROS in G_2/M cell cycle arrest and apoptosis. (**A**) Capan-2 cells were treated with different concentrations of BITC for 24 h and ROS generation was determined by using Fluorescent Hydrogen Peroxide/Peroxidase Detection Kit as described in Materials and Methods as well as using 6-carboxy-2′,7′-dichlorodihydrofluoroscein diacetate by flow cytometry. Capan-2 cells treated with BITC were analyzed for ROS generation (hydrogen peroxide measurement) in a (A) concentration- and (**B**) time-dependent manner. In addition, cells were pre-treated with 5 mM antioxidant NAC for 1 h followed by treatment with or without 10 μM BITC for 24 h and were analyzed for (**C**) ROS generation by flow cytometry; (**D**) cell cycle distribution; (**E**) expression of p-ERK (Thr202/Tyr204), p-JNK (Thr183/Tyr185), p-H2A.X (Ser-139), protein levels of ERK, JNK, P21, Cdc25C, Cdk1, cyclin B1 and cleaved fragments of caspase-3 and PARP and (**F**) apoptosis induction. Each blot was stripped and reprobed with anti-β-actin antibody to ensure equal protein loading. Values are means ± standard errors of the mean of three independent experiments (each conducted in triplicate). Data were analyzed by one-way non-parametric analysis of variance followed by Bonferroni's post hoc multiple comparison test. Differences were considered statistically significant at $^{*}P < 0.05$, $^{**}P < 0.01$ and $^{***}P < 0.001$ when compared with control and $\#P < 0.05$, $\#\#P < 0.01$ and $\#\#\#P < 0.001$ when compared with BITC treatment.

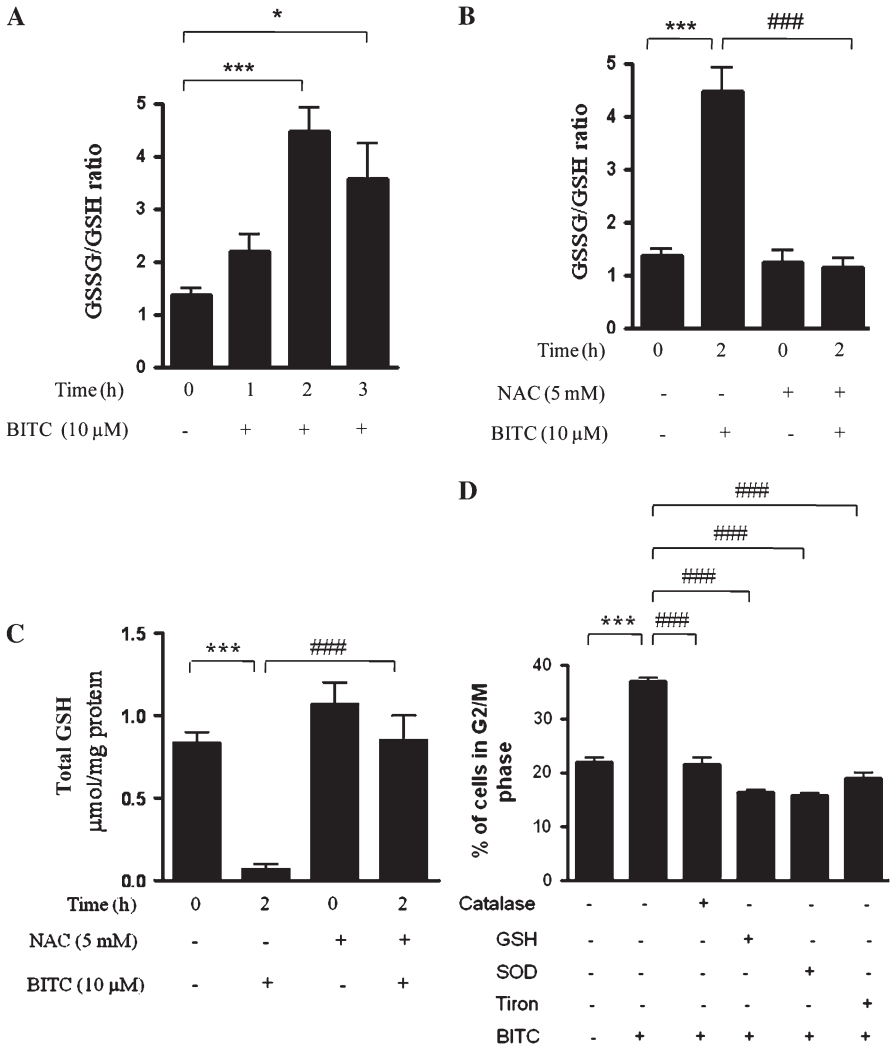

Fig. 5. BITC treatment depletes GSH levels. (**A**) Capan-2 cells were treated with 10 μM BITC for 0, 1, 2 or 3 h and total and oxidized GSH levels were measured as described in Materials and Methods. (**B** and **C**) Cells were pre-treated with 5 mM NAC for 1 h followed by treatment with or without 10 μM BITC for 2 h and oxidized as well as total GSH levels were measured. (**D**) Cells were pre-treated with 5 mM GSH, 5000 U/ml catalase, 5000 U/ml SOD or 10 mM tiron for 1 h followed by treatment with or without 10 μM BITC for 24 h and its effect on the cell cycle distribution was evaluated by flow cytometry as described in Materials and Methods. Values are means ± standard errors of the mean of three independent experiments (each conducted in triplicate). Data were analyzed by one-way non-parametric analysis of variance followed by Bonferroni's post hoc multiple comparison test. Differences were considered statistically significant at $^{*}P < 0.05$, $^{**}P < 0.01$ and $^{***}P < 0.001$ when compared with control and $\#P < 0.05$, $\#\#P < 0.01$ and $\#\#\#P < 0.001$ when compared with BITC treatment.

evaluated the effect of BITC on normal pancreatic HPDE-6 cells. In our previous study, we have demonstrated that normal HPDE-6 cells were almost resistant to the growth inhibitory effects of BITC (18). In the present study, we observed that BITC treatment does not induce any apoptosis in HPDE-6 cells (Figure 6E). Further, BITC failed to cause G_2/M cell cycle arrest in these cells (Figure 6F). We did neither observe any basal phosphorylation levels of ERK, JNK and P38 in HPDE-6 cells nor any change in their protein level after BITC treatment (Figure 6G). BITC treatment failed to cause ROS generation in HPDE-6 cells in a concentration- and time-dependent study (Figure 6H and I). The GSH levels were also not affected by BITC treatment in normal HPDE-6 cells (Figure 6J). These results suggest that normal HPDE-6 cells are almost resistant to the deleterious effects of BITC; nevertheless, the mechanism behind this resistance remains to be elucidated.

Discussion

Epidemiologic studies continue to support the fact that dietary intake of cruciferous vegetables may reduce the risk of different types of malignancies, including pancreatic cancer (4,5,7). BITC, a dietary agent abundant in many cruciferous vegetables, has been shown previously to exert potent anti-proliferative activity (12–16,18,30). Previously, we have shown that BITC induces apoptosis by arresting the cells in G_2/M phase of the cell cycle (16); however, the exact mechanism involved in this process was not clearly understood. In the present study, we demonstrate the generation of ROS leading to the activation of MAPK family members ERK, JNK and P38 resulting in G_2/M cell cycle arrest and apoptosis.

Several investigators have reported the role of MAPK signaling in the regulation of apoptosis in various cancer cells (19,31–38). Our results show that BITC treatment caused very early and sustained activation of MAPK. Interestingly, activation of all the three MAPK family members was not observed in normal HPDE-6 cells. BITC-induced G_2/M cell cycle arrest as well as apoptosis was completely blocked in the cells where ERK activation was pharmacologically inhibited by PD98059 or silenced by MAPK8-shRNA. We also observed that G_2/M regulatory proteins that were modulated by BITC treatment remained unchanged in the cells treated with PD98059 or MAPK8-shRNA, clearly indicating the involvement of ERK

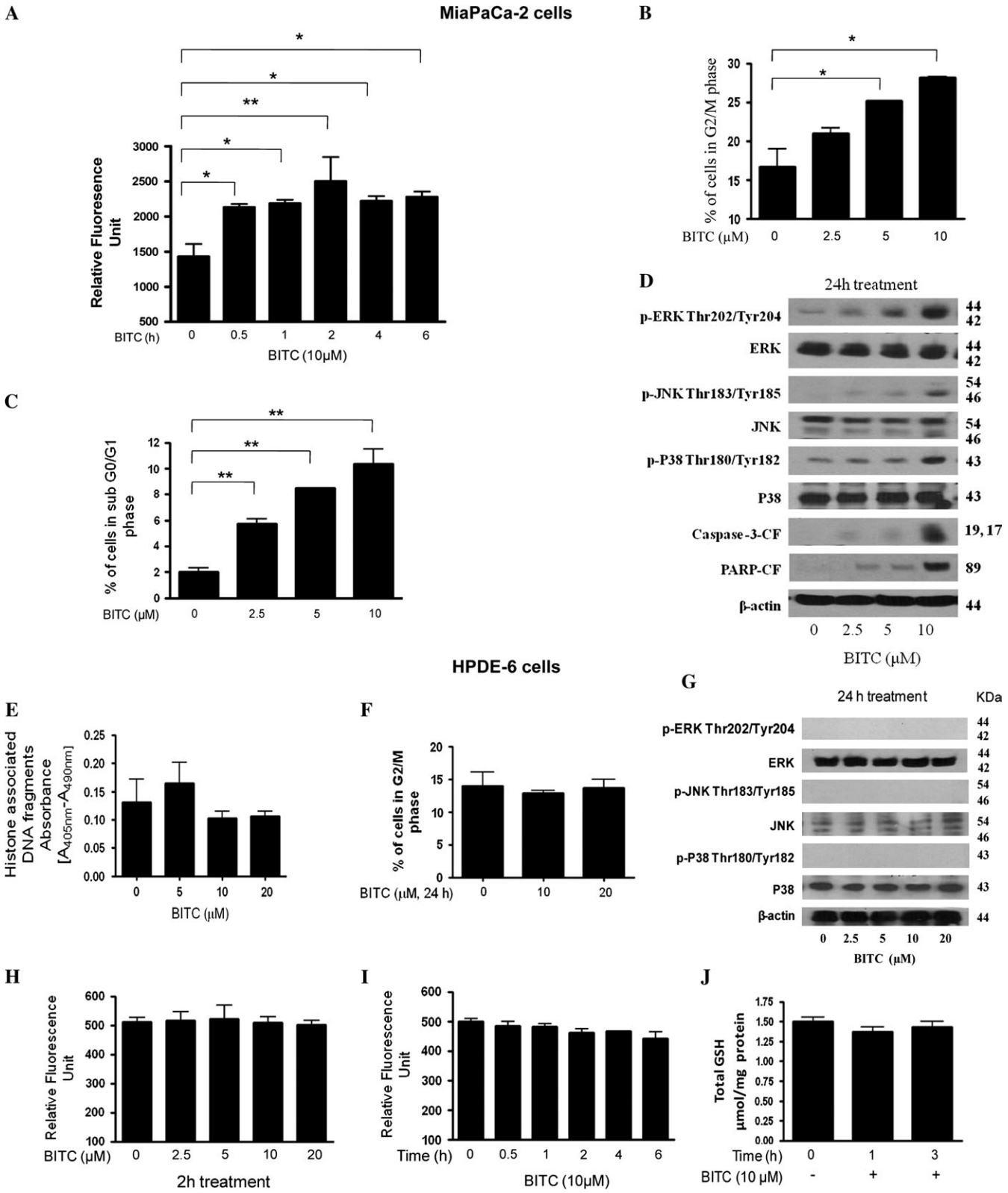

Fig. 6. Effect of BITC on MiaPaCa-2 and normal immortalized HPDE-6 cells. MiaPaCa-2 cells were treated with varying concentrations of BITC for 24 h and were evaluated for (**A**) ROS generation using Hydrogen Peroxide Detection Kit, (**B**) G_2/M cell cycle arrest by flow cytometry, (**C**) apoptosis by flow cytometry and (**D**) expression of p-ERK (Thr202/Tyr204), p-JNK (Thr183/Tyr185) and p-H2A.X (Ser-139), protein levels of ERK and JNK and cleaved fragments of caspase-3 and PARP by western blotting. Normal HPDE-6 cells were treated with varying concentrations of BITC for 24 h and the effect of BITC on (**E**) apoptosis was measured by Cell Death Detection ELISA assay, (**F**) cell cycle distribution by flow cytometry, (**G**) the expression of p-ERK (Thr202/Tyr204), ERK, p-JNK (Thr183/Tyr185), JNK, p-P38 (Thr180/Tyr182) and P38 by western blotting. Same blot was stripped and reprobed with anti-β-actin antibody to ensure equal protein loading. HPDE-6 cells were treated with varying concentrations of BITC for 0–24 h and ROS generation was measured in a (**H**) concentration- and (**I**) time-dependent manner. (**J**) Total GSH level was measured in BITC-treated HPDE-6 cells using a kit. Values are means ± standard errors of the mean of three independent experiments (each conducted in triplicate). Data were analyzed by one-way non-parametric analysis of variance followed by Bonferroni's post hoc multiple comparison test. Differences were considered statistically significant at $^{*}P < 0.05$ and $^{**}P < 0.01$ when compared with control.

activation in BITC-mediated G_2/M cell cycle arrest. Our data are in agreement with the previous reports where ERK activation was involved in cell cycle arrest and apoptosis (10,19,21,22). Several studies have shown the involvement of ERK signaling in regulating apoptosis. Even though ERK delivers a survival signal, few recent studies have correlated the activation of ERK with induction of apoptosis (16,31,33,39,41,42,46). In fact, oxidants have been shown to activate ERK by taking over growth factor receptor signaling pathways (16,31,33,39,41,42,46). In addition, ERK may get activated in response to DNA damage. Our results in agreement demonstrate that BITC treatment results in ROS generation and DNA damage causing activation of ERK leading to G_2/M arrest and apoptosis. However, JNK (SP600125) and P38 (SB202190) inhibitors failed to protect the cells from BITC-mediated G_2/M cell cycle arrest. Our results are in contrast with recent published reports where both ERK and P38 activation was involved in vanadate-induced G_2/M arrest and apoptosis in A549 human lung cancer cells (39). Similarly, Moon *et al.* (40) demonstrated the role of ERK and JNK activation in G_2/M arrest and apoptosis mediated by pextenotoxin in human leukemia cells. Nevertheless, JNK or P38 inhibitors and MAPK8-shRNA almost completely abrogated BITC-induced apoptosis in Capan-2 cells, suggesting the role of all three MAPK members in BITC-induced apoptosis. These results are consistent with several studies where activation of MAPK has been shown to be associated with the induction of apoptosis (41,42). In addition, our studies show that BITC treatment leads to the increased expression of pro-apoptotic protein Bax. Expression of Bax was blocked in the cells transfected with MAPK8-shRNA, indicating that Bax is being regulated by MAPK in our model and is serving as an intermediate signaling molecule and playing role in induction of apoptosis.

ROS are the known mediators of intracellular signaling cascades. Excessive production of ROS nonetheless leads to oxidative stress, loss of cell function and apoptosis or necrosis (19,20,24,43). Induction of apoptosis by BITC via ROS generation has been reported recently (44,45). Consistently, our present studies also show that BITC treatment causes ROS generation in Capan-2 cells that can be blocked by NAC pre-treatment. Moreover, we observed that NAC or tiron pretreatment significantly blocks BITC-mediated G_2/M cell cycle arrest. ROS are also known to play a crucial role in activating various signaling molecules including MAPK (19,20,31,33,39,41,42,46). Moreover, MAPK can get activated in response to DNA damage and regulate expression of G_2/M cell cycle regulatory proteins such as Cdc25C and Cdk1 (40,47,48). ROS are well known to cause DNA damage leading to the activation of MAPK (19). Our results do show that blocking ROS generation by NAC completely blocks DNA damage (phosphorylation of H2A.X at Ser 139), induction of p21 as well as activation of ERK and JNK induced by BITC treatment. On the other hand, NAC treatment failed to block the activation of P38. The modulation of G_2/M regulatory proteins by BITC was also blocked by NAC treatment, thus protecting the cells from BITC-induced G_2/M arrest and apoptosis. However, a study published by Zhang indicated that adding NAC or GSH to the culture medium significantly blocked the uptake of sulforaphane and BITC in murine hepatoma cells (49). It is possible that the effect of NAC we observe in our model may in part be due to inhibition of BITC uptake. We observed that ROS were generated 0.5 h after BITC treatment leading to the activation of ERK and JNK by 1 h and G_2/M arrest and apoptosis by 24 h. We thus established in the present study the involvement of ROS in the activation of ERK and JNK in pancreatic cancer cells. However, BITC-mediated G_2/M cell cycle arrest was specifically mediated through the activation of ERK and not by JNK or P38, whereas apoptosis was mediated via ERK, JNK and P38. Cells with increased ROS generation may depend more on the cellular antioxidant system to keep redox balance, and these cells would be highly sensitive to agents that disable the cellular antioxidant system (20,24–26). On the other hand, normal cells may be able to better tolerate such redox modulation, owing to their low level of basal ROS output and intact metabolic regulation. As such, the redox alterations in pancreatic cancer cells may provide a biological basis for developing new strategy to selective kill the malignant cells. GSH is a key regulator of cell death and survival of cancer cells (27). Besides its direct ROS-scavenging effects, GSH also functions in maintaining redox status of some apoptosis-related proteins (27). Our results show that BITC treatment quickly and substantially decreased the total GSH levels as well as increased the GSSG (oxidized form of GSH) levels, which was prevented by NAC pre-treatment. BITC treatment, however, failed to generate ROS or decrease GSH levels in normal HPDE-6 cells. These results are in agreement with our previous published studies where we demonstrated decline in GSH as a possible mechanism for intracellular redox imbalance leading to ROS generation and induction of apoptosis (20). The decrease in GSH level in Capan-2 cells could be due to the increased conjugation of GSH with BITC, which is a strong electrophile. The conjugate may be formed non-enzymatically or may be mediated enzymatically by GSH *S*-transferase (50), thus decreasing intracellular GSH level. The GSH–isothiocyanate conjugate has been shown to be exported out by transporters such as multidrug resistance protein-2 (51). Our results are in agreement with previous study where rapid accumulation of BITC was observed in murine hepatoma cells resulting in drastic reduction of intracellular GSH levels (49). Apart from GSH, antioxidants such as catalase, SOD and tiron have been shown to scavenge ROS and protect the cells from ROS-mediated apoptosis (28,29). It appears that BITC treatment results in the generation of superoxide radical and hydrogen peroxide in our cell lines. Superoxide radical is reduced to hydrogen peroxide by SOD. On the other hand, hydrogen peroxide is converted to H_2O by catalase. We observed that BITC-mediated G_2/M arrest was significantly blocked by catalase, SOD or tiron, confirming the presence and role of ROS in BITC-induced G_2/M arrest.

Taken together, our results indicate that BITC treatment causes intracellular ROS resulting in the activation of MAPK, which eventually leads to cell cycle arrest and apoptosis in pancreatic cancer cells. The effect of BITC appeared to be specific to pancreatic cancer cells as normal HPDE-6 cells remained unaffected by BITC treatment. However, detailed studies are in progress to delineate the mechanism of the cells' specific effects of BITC.

Supplementary material

Supplementary figure 1 can be found at http://carcin.oxfordjournals.org/

Funding

National Cancer Institute, United States Public Health Service RO1 (CA106953, CA129038) to S.K.S.; Texas Tech University Health Sciences Center, School of Pharmacy to S.K.S.

Acknowledgements

The authors wish to thank Dr Ming-Sound Tsao, University of Toronto, Canada, for providing normal immortal HPDE-6 cells.

Conflict of Interest Statement: None declared.

References

1. Jemal,A. *et al.* (2005) Cancer statistics, 2005. *CA Cancer J. Clin.*, **55**, 10–30.
2. DiGiuseppe,J.A. *et al.* (1996) Molecular biology and the diagnosis and treatment of adenocarcinoma of the pancreas. *Adv. Anat. Pathol.*, **3**, 139–155.
3. DiMagno,E.P. *et al.* (1999) AGA technical review on the epidemiology, diagnosis, and treatment of pancreatic ductal adenocarcinoma. American Gastroenterological Association. *Gastroenterology*, **117**, 464–484.
4. Olsen,G.W. *et al.* (1991) Nutrients and pancreatic cancer: a population-based case-control study. *Cancer Causes Control*, **2**, 291–297.
5. Block,G. *et al.* (1992) Fruit, vegetables and cancer prevention: a review of the epidemiological evidence. *Nutr. Cancer*, **18**, 1–29.
6. Ji,B.T. *et al.* (1995) Dietary factors and risk of pancreatic cancer: a case control study in Shanghai China. *Cancer Epidemiol. Biomarkers Prev.*, **4**, 885–893.

7. Bueno de Mesquita,H.B. *et al*. (1999) Intake of foods and nutrients and cancer of the exocrine pancreas: a population-based case-control study in The Netherlands. *Int. J. Cancer*, **48**, 540–549.
8. Srivastava,S.K. *et al*. (2003) Allyl isothiocyanate, a constituent of cruciferous vegetables, inhibits growth of PC-3 human prostate cancer xenografts *in vivo*. *Carcinogenesis*, **24**, 1665–1670.
9. Xiao,D. *et al*. (2003) Allyl isothiocyanate, a constituent of cruciferous vegetables, inhibits proliferation of human prostate cancer cells by causing G2/M arrest and inducing apoptosis. *Carcinogenesis*, **24**, 891–897.
10. Miyoshi,N. *et al*. (2004) Benzyl isothiocyanate modifies expression of the G2/M arrest-related genes. *Biofactors*, **21**, 23–26.
11. Miyoshi,N. *et al*. (2004) A link between benzyl isothiocyanate-induced cell cycle arrest and apoptosis: involvement of mitogen-activated protein kinases in the Bcl-2 phosphorylation. *Cancer Res.*, **64**, 2134–2142.
12. Srivastava,S.K. *et al*. (2004) Cell cycle arrest and apoptosis-induced by benzyl isothiocyanate are associated with inhibition of nuclear factor kappa B activation in human pancreatic cancer cells. *Carcinogenesis*, **25**, 1701–1709.
13. Zhang,Y. *et al*. (1994) Anticarcinogenic activities of organic isothiocyanates: chemistry and mechanisms. *Cancer Res.*, **54**, S1976–S1981.
14. Stoner,G.D. *et al*. (1997) Isothiocyanates and plant polyphenols as inhibitors of lung and esophageal cancer. *Cancer Lett.*, **114**, 113–119.
15. Hecht,S.S. (1999) Chemoprevention of cancer by isothiocyanates, modifiers of carcinogen metabolism. *J. Nutr.*, **129**, S768–S774.
16. Zhang,R. *et al*. (2006) Benzyl isothiocyanate-induced DNA damage causes G2/M cell cycle arrest and apoptosis in human pancreatic cancer cells. *J. Nutr.*, **136**, 2728–2734.
17. Furukawa,T. *et al*. (1996) Long-term culture and immortalization of epithelial cells from normal adult human pancreatic ducts transfected by the E6E7 gene of human papilloma virus 16. *Am. J. Pathol.*, **148**, 1763–1770.
18. Sahu,R.P. *et al*. (2009) The role of STAT-3 in the induction of apoptosis in pancreatic cancer cells by benzyl isothiocyanate. *J. Natl Cancer Inst.*, **101**, 174–193.
19. Shi,Y. *et al*. (2008) Triphala inhibits both *in vitro* and *in vivo* xenograft growth of pancreatic tumor cells by inducing apoptosis. *BMC Cancer*, **8**, 294.
20. Zhang,R. *et al*. (2008) *In vitro* and *in vivo* induction of apoptosis by capsaicin in pancreatic cancer cells is mediated through ROS generation and mitochondrial death pathway. *Apoptosis*, **13**, 1465–1478.
21. Cho,S.D. *et al*. (2005) Involvement of c-Jun N-terminal kinase in G2/M arrest and caspase-mediated apoptosis induced by sulforaphane in DU145 prostate cancer cells. *Nutr. Cancer*, **52**, 213–224.
22. Ray,G. *et al*. (2006) Modulation of cell-cycle regulatory signaling network by 2-methoxyestradiol in prostate cancer cells is mediated through multiple signal transduction pathways. *Biochemistry*, **45**, 3703–3713.
23. Paolini,M. *et al*. (2004) Induction of cytochrome P450, generation of oxidative stress and *in vitro* cell-transforming and DNA-damaging activities by glucoraphanin, the bioprecursor of the chemopreventive agent sulforaphane found in broccoli. *Carcinogenesis*, **25**, 61–67.
24. Singh,S.V. *et al*. (2005) Sulphoraphane-induced cell death in human prostate cancer cells is initiated by reactive oxygen species. *J. Biol. Chem.*, **280**, 19911–19924.
25. Wu,X.J. *et al*. (2007) Targeting ROS: selective killing of cancer cells by a cruciferous vegetable derived pro-oxidant compound. *Cancer Biol. Ther.*, **6**, 646–647.
26. Choi,W.Y. *et al*. (2008) Sulforaphane generates reactive oxygen species leading to mitochondrial perturbation for apoptosis in human leukemia U937 cells. *Biomed. Pharmacother.*, **62**, 637–644.
27. Ghezzi,P. (2005) Regulation of protein function by glutathionylation. *Free Radic. Res.*, **39**, 573–580.
28. Han,Y.H. *et al*. (2009) Tiron, a ROS scavenger, protects human lung cancer Calu-6 cells against antimycin A-induced cell death. *Oncol. Rep.*, **21**, 253–261.
29. Schreibelt,G. *et al*. (2007) Reactive oxygen species alter brain endothelial tight junction dynamics via RhoA, PI3 kinase, and PKB signaling. *FASEB J.*, **21**, 3666–3676.
30. Zhang,Y. *et al*. (1992) A major inducer of anticarcinogenic protective enzymes from broccoli: isolation and elucidation of structure. *Proc. Natl Acad. Sci. USA*, **89**, 2399–2403.
31. Zhang,X. *et al*. (2003) Reactive oxygen species and extracellular signal-regulated kinase ½ mitogen-activated protein kinase mediate hyperoxia-induced cell death in lung epithelium. *Am. J. Respir. Cell Mol. Biol.*, **28**, 305–315.
32. Ma,Y. *et al*. (2006) Role of nongenomic activation of phosphatidylinositol 3-kinase/Akt and mitogen-activated protein kinase/extracellular signal-regulated kinase kinase/extracellular signal-regulated kinase 1/2 pathway in 1,25D3-mediated apoptosis in squamous cell carcinoma cells. *Cancer Res.*, **66**, 8131–8138.
33. Jeon,E.S. *et al*. (2007) Sphingosylphosphoryl choline induces apoptosis of endothelial cells through reactive oxygen species-mediated activation of ERK. *J. Cell Biochem.*, **100**, 1536–1547.
34. Yu,W. *et al*. (2001) Activation of extracellular signal-regulated kinase and c-Jun-NH(2)-terminal kinase but not p38 mitogen-activated protein kinases is required for RRR-alpha-tocopheryl succinate-induced apoptosis of human breast cancer cells. *Cancer Res.*, **61**, 6569–6576.
35. Choi,Y.J. *et al*. (2003) Sodium orthovanadate potentiates EGCG-induced apoptosis that is dependent on the ERK pathway. *Biochem. Biophys. Res. Commun.*, **305**, 176–185.
36. Xu,C. *et al*. (2006) ERK and JNK signaling pathways are involved in the regulation of activator protein 1 and cell death elicited by three isothiocyanates in human prostate cancer PC-3 cells. *Carcinogenesis*, **27**, 437–445.
37. Shim,H.Y. *et al*. (2007) Acacetin-induced apoptosis of human breast cancer MCF-7 cells involves caspase cascade, mitochondria-mediated death signaling and SAPK/JNK1/2-c-Jun activation. *Mol. Cells*, **24**, 95–104.
38. Filomeni,G. *et al*. (2007) trans-Resveratrol induces apoptosis in human breast cancer cells MCF-7 by the activation of MAP kinases pathways. *Genes Nutr.*, **2**, 295–305.
39. Zhang,Z. *et al*. (2003) Role of reactive oxygen species and MAPKs in vanadate-induced G(2)/M phase arrest. *Free Radic. Biol. Med.*, **34**, 1333–1342.
40. Moon,D.O. *et al*. (2008) Induction of G2/M arrest, endoreduplication, and apoptosis by actin depolymerization agent pextenotoxin-2 in human leukemia cells, involving activation of ERK and JNK. *Biochem. Pharmacol.*, **76**, 312–321.
41. Kim,H.J. *et al*. (2006) N-(4-hydroxyphenyl) retinamide-induced apoptosis triggered by reactive oxygen species is mediated by activation of MAPKs in head and neck squamous carcinoma cells. *Oncogene*, **25**, 2785–2794.
42. Kim,K.W. *et al*. (2009) Silibinin inhibits glioma cell proliferation via Ca(2+)/ROS/MAPK-dependent mechanism *in vitro* and glioma tumor growth *in vivo*. *Neurochem. Res.*, **34**, 1479–1490.
43. Mclean,L. *et al*. (2008) Aminoflavone induces oxidative DNA damage and reactive oxidative species-mediated apoptosis in breast cancer cells. *Int. J. Cancer*, **22**, 1665–1674.
44. Nakamura,Y. *et al*. (2002) Involvement of the mitochondrial death pathway in chemopreventive benzyl isothiocyanate-induced apoptosis. *J. Biol. Chem.*, **277**, 8492–8499.
45. Xiao,D. *et al*. (2008) Benzyl isothiocyanate targets mitochondrial respiratory chain to trigger reactive oxygen species-dependent apoptosis in human breast cancer cells. *J. Biol. Chem.*, **283**, 30151–30163.
46. Hsu,W.H. *et al*. (2007) Berberine induces apoptosis in SW620 human colonic carcinoma cells through generation of reactive oxygen species and activation of JNK/p38 MAPK and FasL. *Arch. Toxicol.*, **81**, 719–728.
47. Tang,D. *et al*. (2002) ERK activation mediates cell cycle arrest and apoptosis after DNA damage independent of p53. *J. Biol. Chem.*, **277**, 12710–12717.
48. Lee,J.H. *et al*. (2007) Regulation of cyclin-dependent kinase 5 and p53 by ERK1/2 pathway in the DNA damage-induced neuronal death. *J. Cell Physiol.*, **210**, 784–797.
49. Zhang,Y. (2000) Role of glutathione in the accumulation of anticarcinogenic isothiocyanates and their glutathione conjugates by murine hepatoma cells. *Carcinogenesis*, **21**, 1175–1182.
50. Hu,Y. *et al*. (2007) Glutathione- and thioredoxin-related enzymes are modulated by sulfur-containing chemopreventive agents. *Biol. Chem.*, **388**, 1069–1081.
51. Bauer,B. *et al*. (2008) Coordinated nuclear receptor regulation of the efflux transporter, Mrp2, and the phase-II metabolizing enzyme, GSTpi, at the blood-brain barrier. *J. Cereb. Blood Flow Metab.*, **28**, 1222–1234.

Received March 24, 2009; revised June 15, 2009; accepted June 16, 2009